ChemComm

COMMUNICATION

View Article Online
View Journal | View Issue

Cite this: *Chem. Commun.*, 2019, 55, 14430

Received 12th September 2019,
Accepted 29th October 2019

DOI: 10.1039/c9cc07153a

rsc.li/chemcomm

Dynamic host–guest interaction enables autonomous single molecule blinking and super-resolution imaging†

Ranjan Sasmal,[a] Nilanjana Das Saha,[ab] Florian Schueder,[cd] Divyesh Joshi,[e] Vasu Sheeba,[f] Ralf Jungmann[cd] and Sarit S. Agasti*[ab]

Synthetic host–guest complexes are inherently dynamic as they employ weak and reversible noncovalent interactions for their recognition processes. We strategically exploited dynamic supramolecular recognition between fluorescently labeled guest molecules to complementary cucurbit[7]uril hosts to obtain stochastic switching between fluorescence ON- and OFF-states, enabling PAINT-based nanoscopic imaging in cells and tissues.

Supramolecular chemistry facilitates the engineering of molecular systems by the incorporation of non-covalent recognition motifs. Among various non-covalent building blocks, host–guest systems are of specific interest due to their high levels of chemoselectivity, particularly for recognition processes in aqueous media.[1–4] The benefit of employing a host–guest system in engineering molecular systems arises from the highly selective yet reversible nature of their interaction. This dynamic interaction allows designing an approach to control the properties of the systems in a manner that is programmable, modular, and responsive. These features have been emphasized in several applications, including functional materials,[5–9] catalysis,[10,11] sensing,[12–14] imaging[15,16] and therapeutics.[17–23]

Super-resolution fluorescence microscopy is a powerful tool for the visualization of molecular organization beyond the diffraction limit of light.[24–26] PAINT (points accumulation for imaging in nanoscale topography) represents an easy-to-implement concept to perform such super-resolution microscopy.[27–29] A PAINT based strategy benefits from the use of conventional fluorophores and importantly, the implementation of PAINT does not require any specialized equipment or experimental conditions. Initially, PAINT was implemented using non-specifically interacting dye molecules,[27] which hindered the use of this strategy for imaging any specific target of interest. Recently, to achieve specificity, PAINT probes were developed by exploiting macromolecular recognition processes. Most notable examples are DNA and protein-fragment based probes, called DNA-PAINT and IRIS.[30,31] However, achieving such specificity from small molecular probes remains challenging. Notably, small molecular probes offer several benefits for PAINT, including minimal localization offset, high labeling density, live cell imaging capability, and ability to tag and image molecules that are beyond genetic tagging.

Herein, we introduce a new class of small synthetic PAINT probes using highly specific yet dynamic interaction between synthetic host–guest pairs. We developed the dynamic probe for super-resolution imaging using cucurbit[7]uril (CB[7]) based synthetic recognition pairs. We selected CB[7] for this study in view of its ability to form specific inclusion complexes with a variety of guest molecules in the biological medium with affinities (K_a, association constant) that vary from 10^3 to 10^{15} M^{-1}.[32–39] Importantly, considering close to diffusion-controlled association rate ($k_{on} \sim 10^8$ M^{-1} s^{-1}), such a wide affinity range allows programmable tuning of the binding time (τ_b, where τ_b = 1/dissociation rate (k_{off})) of CB[7] dynamic host–guest complexation events[40–43] The key aspect of our imaging strategy was the utilization of this programmable control over the binding events through proper selection of guest molecules to obtain stochastic switching between fluorescence ON- and OFF-states at single-molecule resolution. We demonstrate that the fluorescently labeled hexamethylenediamine (HMD) guest is capable of providing the necessary fluorescent blinking with prescribed brightness and frequency *via* dynamic complexation with CB[7] to enable two-dimensional (2D) and 3D super-resolution imaging of biomolecules with >10× better resolution than the diffraction limited imaging. We show that the autonomous blinking feature along with the capability of a host–guest

[a] *New Chemistry Unit, Jawaharlal Nehru Centre for Advanced Scientific Research (JNCASR), Bangalore, Karnataka 560064, India. E-mail: sagasti@jncasr.ac.in*
[b] *Chemistry & Physics of Materials Unit, Jawaharlal Nehru Centre for Advanced Scientific Research (JNCASR), Bangalore, Karnataka 560064, India*
[c] *Max Planck Institute of Biochemistry, 82152 Martinsried near Munich, Germany*
[d] *Department of Physics and Center for Nanoscience, Ludwig Maximillian University, 80539 Munich, Germany*
[e] *Molecular Biology and Genetics Unit, Jawaharlal Nehru Centre for Advanced Scientific Research (JNCASR), Bangalore, Karnataka 560064, India*
[f] *Neuroscience Unit, Jawaharlal Nehru Centre for Advanced Scientific Research (JNCASR), Bangalore, Karnataka 560064, India*

† Electronic supplementary information (ESI) available. See DOI: 10.1039/c9cc07153a

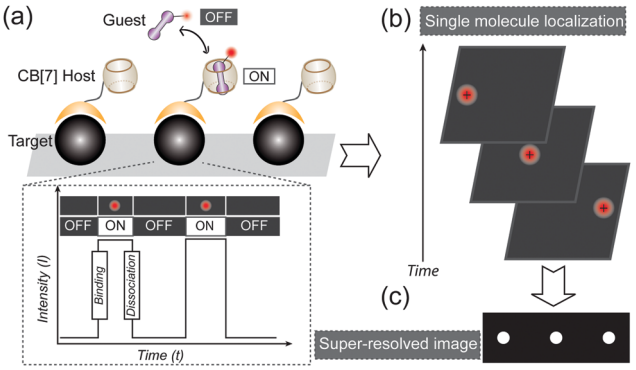

Fig. 1 Concept of host–guest mediated super-resolution imaging. (a) The fluorophore conjugated guest molecule interacts transiently with CB[7] docking sites to produce fluorescence blinking. (b) Accurate coordinates of the molecules in the ON-state are determined by fitting the point-spread function (PSF) to a Gaussian function. (c) Accumulation of coordinates from all the frames provides an image representing the organization of molecules in nanometer resolution.

complex to maintain recognition specificity in the complexities of the intracellular environment allows this imaging method to be applicable for live-cell super-resolution microscopy.

The strategy for real-time probing of the dynamic host–guest interaction is shown in Fig. 1, which provides the basis for super-resolution imaging. There are two important components in this technique: the CB[7] conjugated targeting ligand and the guest molecule conjugated fluorophore (the 'imager'). Through specific interaction (*e.g.*, antigen–antibody), the targeting ligand places the CB[7] host onto the biomolecule of interest. When a guest imager is introduced into the medium it interacts transiently with CB[7] docking sites displayed on the surface of target biomolecules through host–guest interaction. The host–guest interaction is driven by weak non-covalent interactions. These interactions are not sufficiently strong to withstand thermal motions that pull the complexes apart, leading to the dissociation of the complex. In the unbound state, the free-floating imager only leads to background fluorescence (OFF state), whereas a bright fluorescence (ON state) is detected upon transient immobilization of the imager onto the target biomolecule through host–guest interaction with CB[7]. The transient immobilization of the guest molecule allows localization of its position with nanometer precision *via* PAINT.[27] These coordinates can then be used to reconstruct a super-resolved image of the biomolecule of interest.

In order to employ CB[7] for super-resolution imaging, it was first conjugated with targeting ligands. For this purpose, we first derivatized CB[7] with amine functionality in three steps.[44] CB[7] with amine functionality was subsequently conjugated with *trans*-cyclooctene (TCO). The TCO click handle was used to attach CB[7] with tetrazine conjugated primary targeting ligands, including antibodies and small molecules (Scheme S5a, ESI†).[15] A crucial consideration while developing this imaging strategy was to find suitable guest molecules that provide an appropriate length of binding events and ensure collection of sufficient number of photons for precise single-molecule localization of the binding events. Guest molecules with very long residence time (*i.e.*, binding time, τ_b) will result in overlapping single molecule events, whereas guest molecules with very short residence time will produce fewer photons, resulting in reduced resolution and image quality. To search for the appropriate imager, a set of three different guest molecules with varying K_a was explored: propylamine (10^3–10^4 M^{-1}), HMD (10^6–10^7 M^{-1}), and adamantylamine (ADA, 10^{12}–10^{13} M^{-1}).[45] Considering the literature reported k_{on} as 10^8 M^{-1} s^{-1}, the residence times for the CB[7] host with propylamine, HMD, and ADA guests were calculated to be around 0.01–0.001 ms, 10–100 ms, and 10^7–10^8 ms, respectively (see the ESI† for calculation).[40–43]

We used the CB[7] immobilized glass surface as an *in vitro* system to investigate the blinking properties of the Alexa Fluor 647 conjugated guest molecules (Fig. S34, ESI†). The propylamine guest, having the lowest affinity, did not generate any detectable fluorescence spots throughout the recording time, presumably due its very short binding time with CB[7] (Fig. S37, ESI†). On the other hand, the use of the very high affinity ADA guest molecule resulted in stable association of the fluorophore with CB[7], as concluded from the initial appearance of high density fluorescence spots that bleached irreversibly over time (Fig. S39, ESI†). However, in the case of the HMD guest, fluorescence intensity traces show autonomous ON/OFF switching of fluorescence (Fig. 2 and Fig. S41, ESI†). The blinking events persisted throughout the recording time, demonstrating transient and repetitive association of the HMD guest with CB[7]. Overall, the *in vitro* experiments indicate that the CB[7]-HMD pair possesses the necessary binding affinity to provide fluorescence blinking with prescribed brightness and frequency to enable precise single-molecule localization.

To translate the host–guest mediated blinking to super-resolution imaging in cells, we used microtubules as an imaging target. Microtubules in Mouse embryonic fibroblast (MEF) cells were stained using primary antibodies against α-tubulin followed by CB[7] conjugated secondary antibodies. 1 nM solution of the HMD guest conjugated Cy5 (HMD-Cy5) imager was added to the cells for recording images. As shown in Fig. S44 (ESI†), the autonomous and stochastic appearance of fluorescent bursts from single molecules as a result of transient host–guest binding events was observed from the cells in PBS buffer without any additives. The average fluorescence ON time is estimated to be ~121 ms (Fig. S45, ESI†). As the imager molecules were continuously replenished from solution, we did not observe any photobleaching during imaging. The spontaneous blinking events continued for hours of imaging under excitation illumination. Images acquired using ~0.138 kW cm^{-2} laser power and

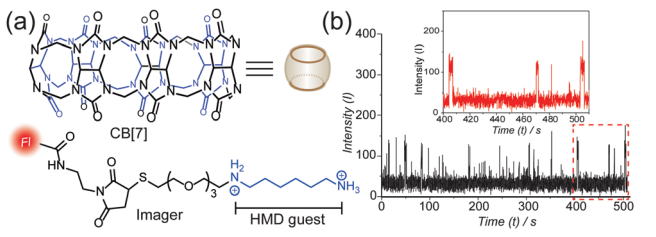

Fig. 2 Fluorescence blinking *via* host–guest interaction. (a) Structure of the CB[7] host and guest imager. (b) Fluorescence trace analysis of a localized spot derived from the CB[7]-immobilized surface shows transient and repetitive binding events throughout the recording time.

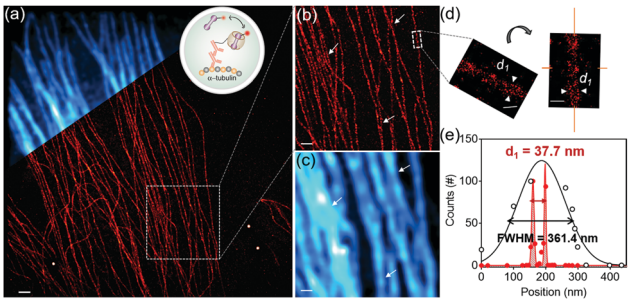

Fig. 3 Super-resolution imaging of microtubules using host–guest interaction. (a) The super-resolved image shows much thinner microtubules as compared to their diffraction-limited counterpart (top left corner). (b) A magnified view of the selected region in a; showing clearly resolved microtubule filaments. (c) Diffraction-limited image of the same region shows indistinguishable filaments. (d) In a highly zoomed-in view of the selected region in b, a single microtubule is observed as two lines due to its hollow structure. (e) The cross-sectional histogram shows a separation of 37.7 nm between the lines (microtubule diameter). Scale bars: (a) 1 μm, (b and c) 500 nm, and (d) 100 nm.

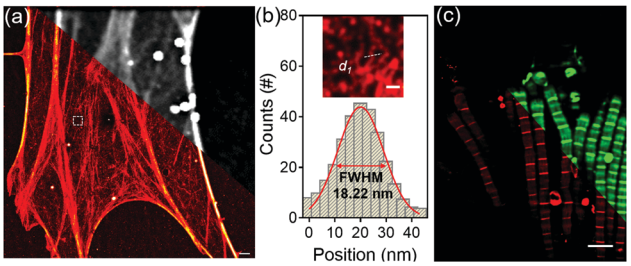

Fig. 4 Super-resolution imaging of F-actin in cells and tissues. (a) Super-resolved image obtained from the host–guest blinking technique resolved individual actin filaments as compared to the conventional diffraction limited image (top right corner). (b) Cross-section profile of a single filament (d_1) shows a FWHM of 18.22 nm. (c) Host–guest interaction mediated super-resolution image of F-actin in thoracic muscle tissues (top right corner shows the diffracted limited image). Scale bars: (a) 1 μm, (b) 100 nm, and (c) 5 μm.

integrated over 50 ms of timescale showed a collection of ~505 photons per frame (Fig. S44g, ESI†). To construct a super-resolved image from the cells, the localizations of the fluorescent molecules were determined with nanometer precision by fitting the point spread function (PSF) to a 2D Gaussian function. Finally coordinates from all the frames were accumulated to construct an overall super-resolution image. In addition, we have implemented a drift correction using gold nanoparticles (~100 nm) as a fiducial marker. Fig. 3a–d clearly demonstrate that the image from host–guest blinking yields a much-improved resolution as compared to their diffraction-limited counterpart. To quantitatively highlight the improvement, the transverse profile of localization of a single microtubule filament was examined. Importantly, host–guest blinking based imaging was able to clearly resolve the hollow cylindrical structure of the microtubule filament with a diameter of ~38 nm (Fig. 3e and Fig. S47, ESI†). On the other hand, the microtubule from the standard diffraction-limited image appeared as one peak with a FWHM of ~361 nm, clearly highlighting the enhanced resolution from host–guest imaging. To achieve 3D super-resolution imaging, we have applied a PSF engineering approach by introducing a phase ramp over one-half of the detection beam path with a glass wedge.[46] Fig. S48 (ESI†) shows a reconstructed super-resolved image of the 3D mitochondrial network over a depth of 1.2 μm. Both horizontal and vertical cross-sections revealed the 3D contour of the hollow-shaped mitochondrial outer membrane. Importantly, host–guest blinking mediated 3D imaging was able to resolve the hollowness of the mitochondria that are as small as 137 nm in diameter, demonstrating the significant improvement of resolution in the *z* direction due to imaging compared to a standard diffraction-limited system.

The smaller footprints of small molecule-based targeting ligands as compared to the antibodies are ideally suited to achieve high density labelling for improved resolution. To demonstrate host–guest based imaging based on a small molecular targeting ligand, we used phalloidin as a highly specific small molecular binder for F-actin and conjugated it to CB[7]. Autonomous blinking was immediately observed upon addition of the HMD-Cy5 imager to a cell that was labeled with phalloidin-conjugated CB[7] (see Fig. S49 and Movie S1, ESI†). We detected an average of ~681 photons per frame using ~0.392 kW cm^{-2} excitation laser power density (integration time 50 ms, Fig. S50a, ESI†). A lateral localization precision of ~13 nm (Fig. S50b, ESI†) was achieved by fitting the PSF to a 2D Gaussian function. Upon reconstruction, individual small actin filaments were clearly resolved in the super-resolved image using the host–guest blinking technique; by contrast, filaments were impossible to distinguish in the diffraction-limited image (Fig. 4a). The measurement of the cross-section of a single filament, as shown in Fig. 4b, exhibited a FWHM of ~18 nm. Similar to the cell culture experiment, specific autonomous blinking was also observed upon addition of the imager to the *Drosophila melanogaster* thoracic muscle tissues. The reconstructed super-resolution image provided a much better view of the actin network from muscle tissues (Fig. 4c and Fig. S51, ESI†), clearly indicating the selectivity of the host–guest based system for nanoscopic imaging in the diversity and complexity of tissue specimens.

To translate host–guest blinking to live-cell imaging, we first used a nanoparticle vector to deliver a phalloidin-CB[7] conjugate to the cytosolic environment.[15] Cells were subsequently incubated with the cell permeable SiR-labeled HMD imager. We observed spontaneous blinking from the intracellular environment, indicating specific interaction of the SiR-labeled HMD imager with the CB[7] host in live cells (see Movie S2, ESI†). The super-resolved image of phalloidin labeled actin fibers, reconstructed from a 60 s recording time, is shown in Fig. 5. The corresponding diffraction limited image clearly indicates the capability of the host–guest probe to enhance resolution in the context of live cell imaging. The super-resolution image yielded an apparent width of 46.6 nm (FWHM) for the actin filament, whereas the standard diffraction limited image shows a FWHM of 345.1 nm for the same filament (Fig. 5). We continuously acquired blinking images for 10 min to construct multiple super-resolution snap-shots. Movie S3 (ESI†) shows a time-lapse video of reconstructed super-resolution snapshots where actin fibers are visible with improved resolution. These results clearly establish the potential of the host–guest based imaging technique in live-cell super-resolution microscopy.

In conclusion, we demonstrated the use of the transient interaction between synthetic host–guest molecules to obtain

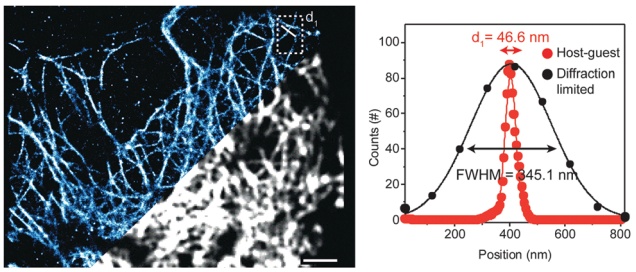

Fig. 5 Super-resolved image of actin from live cells and the corresponding diffraction limited image (bottom right). The cross-section profile of an actin filament (d_1) shows a FWHM of 46.6 nm for the super-resolved image as compared to 345.1 nm for the diffraction limited image. Scale bar: 5 μm.

fluorescence blinking for super-resolution imaging of biomolecules. We showed that the CB[7] host and the HMD guest maintain their interaction specificity even in the complexity of the intracellular environment of a living cell to facilitate the application of host–guest based blinking in live-cell super-resolution microscopy, significantly expanding the scope of host–guest chemistry in *in vivo* biological imaging. We also anticipate that this method will be applicable to study the growth of supramolecular polymers or probing living supramolecular polymerization processes.

S. S. A. acknowledges support by the Wellcome Trust/DBT India Alliance fellowship (IA/I/16/1/502368), the DBT-IYBA Award (BT/09/IYBA/2015/15), and the SERB-ECR Award (ECR/2016/002052). R. J. acknowledges support by the German Research Foundation through the Emmy Noether Program (no. DFG JU 2957/1-1), the SFB1032 (project no. A11), the European Research Council through an ERC Starting Grant (MolMap; grant agreement no. 680241) and the Max Planck Society. We thank Sushma Rao for preparing tissue samples and Prof. V. M. Rotello (UMass-Amherst) for critical comments.

Conflicts of interest

A patent has been filed based on this article.

References

1 R. N. Dsouza, U. Pischel and W. M. Nau, *Chem. Rev.*, 2011, **111**, 7941–7980.
2 L. Jason, M. Pritam, C. Sriparna and I. Lyle, *Angew. Chem., Int. Ed.*, 2005, **44**, 4844–4870.
3 Z. Hirani, H. F. Taylor, E. F. Babcock, A. T. Bockus, C. D. Varnado, C. W. Bielawski and A. R. Urbach, *J. Am. Chem. Soc.*, 2018, **140**, 12263–12269.
4 M. Raeisi, K. Kotturi, I. del Valle, J. Schulz, P. Dornblut and E. Masson, *J. Am. Chem. Soc.*, 2018, **140**, 3371–3377.
5 S. Zhang, Z. Domínguez, K. I. Assaf, M. Nilam, T. Thiele, U. Pischel, U. Schedler, W. M. Nau and A. Hennig, *Chem. Sci.*, 2018, **9**, 8575–8581.
6 L. Zou and M. J. Webber, *Chem. Commun.*, 2019, **55**, 9931–9934.
7 J. d. Barrio, J. Liu, R. A. Brady, C. S. Y. Tan, S. Chiodini, M. Ricci, R. Fernández-Leiro, C.-J. Tsai, P. Vasileiadi, L. Di Michele, D. Lairez, C. Toprakcioglu and O. A. Scherman, *J. Am. Chem. Soc.*, 2019, **141**, 14021–14025.
8 S. Sankaran, M. C. Kiren and P. Jonkheijm, *ACS Nano*, 2015, **9**, 3579–3586.
9 F. Tian, D. Jiao, F. Biedermann and O. A. Scherman, *Nat. Commun.*, 2012, **3**, 1207.
10 J. A. Finbloom, K. Han, C. C. Slack, A. L. Furst and M. B. Francis, *J. Am. Chem. Soc.*, 2017, **139**, 9691–9697.
11 C. J. Bruns, H. Liu and M. B. Francis, *J. Am. Chem. Soc.*, 2016, **138**, 15307–15310.
12 A. Hennig, H. Bakirci and W. M. Nau, *Nat. Methods*, 2007, **4**, 629.
13 N. Amir, A. Zahra and W. M. Nau, *Angew. Chem., Int. Ed.*, 2015, **54**, 792–795.
14 A. T. Bockus, L. C. Smith, A. G. Grice, O. A. Ali, C. C. Young, W. Mobley, A. Leek, J. L. Roberts, B. Vinciguerra, L. Isaacs and A. R. Urbach, *J. Am. Chem. Soc.*, 2016, **138**, 16549–16552.
15 R. Sasmal, N. Das Saha, M. Pahwa, S. Rao, D. Joshi, M. S. Inamdar, V. Sheeba and S. S. Agasti, *Anal. Chem.*, 2018, **90**, 11305–11314.
16 K. L. Kim, G. Sung, J. Sim, J. Murray, M. Li, A. Lee, A. Shrinidhi, K. M. Park and K. Kim, *Nat. Commun.*, 2018, **9**, 1712.
17 L. Zou, A. S. Braegelman and M. J. Webber, *ACS Cent. Sci.*, 2019, **5**, 1035–1043.
18 S. K. Samanta, J. Quigley, B. Vinciguerra, V. Briken and L. Isaacs, *J. Am. Chem. Soc.*, 2017, **139**, 9066–9074.
19 C. Kim, S. S. Agasti, Z. Zhu, L. Isaacs and V. M. Rotello, *Nat. Chem.*, 2010, **2**, 962–966.
20 N. Basílio and U. Pischel, *Chem. – Eur. J.*, 2016, **22**, 15208–15211.
21 M. A. Romero, R. J. Fernandes, A. J. Moro, N. Basílio and U. Pischel, *Chem. Commun.*, 2018, **54**, 13335–13338.
22 Y.-F. Ding, J. Wei, S. Li, Y.-T. Pan, L.-H. Wang and R. Wang, *ACS Appl. Mater. Interfaces*, 2019, **11**, 28665–28670.
23 Q. Huang, K. I. Kuok, X. Zhang, L. Yue, S. M. Y. Lee, J. Zhang and R. Wang, *Nanoscale*, 2018, **10**, 10333–10336.
24 J. B. Grimm, B. P. English, H. Choi, A. K. Muthusamy, B. P. Mehl, P. Dong, T. A. Brown, J. Lippincott-Schwartz, Z. Liu, T. Lionnet and L. D. Lavis, *Nat. Methods*, 2016, **13**, 985.
25 J. Bucevičius, J. Keller-Findeisen, T. Gilat, S. W. Hell and G. Lukinavičius, *Chem. Sci.*, 2019, **10**, 1962–1970.
26 M. Mund, J. A. van der Beek, J. Deschamps, S. Dmitrieff, P. Hoess, J. L. Monster, A. Picco, F. Nédélec, M. Kaksonen and J. Ries, *Cell*, 2018, **174**, 884–896.
27 A. Sharonov and R. M. Hochstrasser, *Proc. Natl. Acad. Sci. U. S. A.*, 2006, **103**, 18911–18916.
28 I. Schoen, J. Ries, E. Klotzsch, H. Ewers and V. Vogel, *Nano Lett.*, 2011, **11**, 4008–4011.
29 N. G. Bozhanova, M. S. Baranov, N. V. Klementieva, K. S. Sarkisyan, A. S. Gavrikov, I. V. Yampolsky, E. V. Zagaynova, S. A. Lukyanov, K. A. Lukyanov and A. S. Mishin, *Chem. Sci.*, 2017, **8**, 7138–7142.
30 R. Jungmann, M. S. Avendaño, J. B. Woehrstein, M. Dai, W. M. Shih and P. Yin, *Nat. Methods*, 2014, **11**, 313–318.
31 T. Kiuchi, M. Higuchi, A. Takamura, M. Maruoka and N. Watanabe, *Nat. Methods*, 2015, **12**, 743.
32 K. I. Assaf and W. M. Nau, *Chem. Soc. Rev.*, 2015, **44**, 394–418.
33 X. Zhou, X. Su, P. Pathak, R. Vik, B. Vinciguerra, L. Isaacs and J. Jayawickramarajah, *J. Am. Chem. Soc.*, 2017, **139**, 13916–13921.
34 D.-W. Lee, K. M. Park, M. Banerjee, S. H. Ha, T. Lee, K. Suh, S. Paul, H. Jung, J. Kim, N. Selvapalam, S. H. Ryu and K. Kim, *Nat. Chem.*, 2011, **3**, 154–159.
35 P. Neirynck, J. Brinkmann, Q. An, D. W. J. van der Schaft, L.-G. Milroy, P. Jonkheijm and L. Brunsveld, *Chem. Commun.*, 2013, **49**, 3679–3681.
36 H. H. L. Lee, C. E. Heo, N. Seo, S. G. Yun, H. J. An and H. I. Kim, *J. Am. Chem. Soc.*, 2018, **140**, 16528–16534.
37 N. Dubel, S. Liese, F. Scherz and O. Seitz, *Angew. Chem., Int. Ed.*, 2019, **58**, 907–911.
38 S.-R. Wang, Y.-Y. Song, L. Wei, C.-X. Liu, B.-S. Fu, J.-Q. Wang, X.-R. Yang, Y.-N. Liu, S.-M. Liu, T. Tian and X. Zhou, *J. Am. Chem. Soc.*, 2017, **139**, 16903–16912.
39 I. Neira, M. D. García, C. Peinador and A. E. Kaifer, *J. Org. Chem.*, 2019, **84**, 2325–2329.
40 C. Bohne, *Chem. Soc. Rev.*, 2014, **43**, 4037–4050.
41 H. Tang, D. Fuentealba, Y. H. Ko, N. Selvapalam, K. Kim and C. Bohne, *J. Am. Chem. Soc.*, 2011, **133**, 20623–20633.
42 C. Márquez, R. R. Hudgins and W. M. Nau, *J. Am. Chem. Soc.*, 2004, **126**, 5806–5816.
43 R. Jungmann, C. Steinhauer, M. Scheible, A. Kuzyk, P. Tinnefeld and F. C. Simmel, *Nano Lett.*, 2010, **10**, 4756–4761.
44 M. M. Ayhan, H. Karoui, M. Hardy, A. Rockenbauer, L. Charles, R. Rosas, K. Udachin, P. Tordo, D. Bardelang and O. Ouari, *J. Am. Chem. Soc.*, 2015, **137**, 10238–10245.
45 S. J. Barrow, S. Kasera, M. J. Rowland, J. del Barrio and O. A. Scherman, *Chem. Rev.*, 2015, **115**, 12320–12406.
46 D. Baddeley, M. B. Cannell and C. Soeller, *Nano Res.*, 2011, **4**, 589–598.